ResearchGate

See discussions, stats, and author profiles for this publication at: https://www.researchgate.net/publication/348575169

User Intent Estimation during robot learning using Physical Human Robot Interaction Primitives

Preprint · January 2021

CITATIONS
0

READS
78

4 authors:

Yujun Lai
University of Technology Sydney
10 PUBLICATIONS **13** CITATIONS
SEE PROFILE

Gavin Paul
University of Technology Sydney
78 PUBLICATIONS **605** CITATIONS
SEE PROFILE

Yunduan Cui
Chinese Academy of Sciences
37 PUBLICATIONS **293** CITATIONS
SEE PROFILE

Takamitsu Matsubara
Nara Institute of Science and Technology
142 PUBLICATIONS **1,446** CITATIONS
SEE PROFILE

Some of the authors of this publication are also working on these related projects:

3D Printing in Construction View project

Revolutionising Mineral Separation using Additive Manufacturing View project

All content following this page was uploaded by Yujun Lai on 18 January 2021.

The user has requested enhancement of the downloaded file.

Autonomous Robots manuscript No.
(will be inserted by the editor)

User Intent Estimation during robot learning using Physical Human Robot Interaction Primitives

Yujun Lai · Gavin Paul · Yunduan Cui · Takamitsu Matsubara

Received: date / Accepted: date

Abstract As robotic systems transition from traditional setups to collaborative workspaces, the prevalence of physical Human Robot Interaction has risen in both industrial and domestic environments. A popular representation for robot behavior is movement primitives which learn, imitate, and generalize from expert demonstrations. While there are existing works in context-aware movement primitives, they are usually limited to contact-free human robot interactions.

This paper presents physical Human Robot Interaction Primitives (pHRIP), which utilize only the interaction forces between the human user and robot to estimate user intent and generate the appropriate robot response during physical human robot interactions.

The efficacy of pHRIP is evaluated through multiple experiments based on target-directed reaching and obstacle avoidance tasks using a real seven degree of freedom robot arm. The results are validated against traditional movement primitives using observations of robotic trajectories, with discussions of future pHRI applications utilizing pHRIP.

Keywords Physical Human-Robot Interaction · Learning from Demonstration

Y. Lai & G. Paul
Centre for Autonomous Systems (UTS:CAS),
University for Technology Sydney, Australia
E-mail: yujun.lai@uts.edu.au

Y. Cui
Center for Automotive Electronics,
Shenzhen Institutes of Advanced Technology,
Chinese Academy of Sciences, Shenzhen, China

T. Matsubara
Robot Learning Lab,
Nara Institute of Science and Technology,
Ikoma, Nara, Japan

1 Introduction

Traditional robots rely on their accuracy, reliability, and strength to perform tasks. However, the variety of tasks performed with a single robot is generally constrained due to financial and time costs to adapt or replace its current program. The same costs exist for control methods that achieve safe Human Robot Interaction (HRI) using industrial robots with fine parameter tuning and heavily pre-determined environments [14].

Recent advances in collaborative robots have paved the way for current research in collaborative interactions between humans and robots due to their inherent safety and improvements in productivity [5]. The increasing adoption of collaborative robots has also boosted the prevalence of HRI applications in both industrial and domestic environments. Physical Human-Robot Interactions (pHRI) is a sub-field of research which includes interactions with direct physical contact or an exchange of forces with a robotic system. Applications with pHRI aim to augment the dexterity of human operators with the precision and repeatability of robotic systems to achieve various tasks, with common applications in haptic feedback [9], disturbance categorization [19], and system stabilization [15].

To improve the robustness of robots in collaborative workspaces, the ability to learn, generalize, and adapt to different tasks is crucial. Two umbrella terms for frameworks which employ expert-learner techniques to generalize robotic motions to different tasks are *Programming by Demonstration* (PbD) [4] and *Learning from Demonstration* (LfD) [1]. Task-oriented measures are regularly used to tackle variability exhibited by human users during pHRI applications [8,20,31]. However, for non-expert users, these measures may degrade the

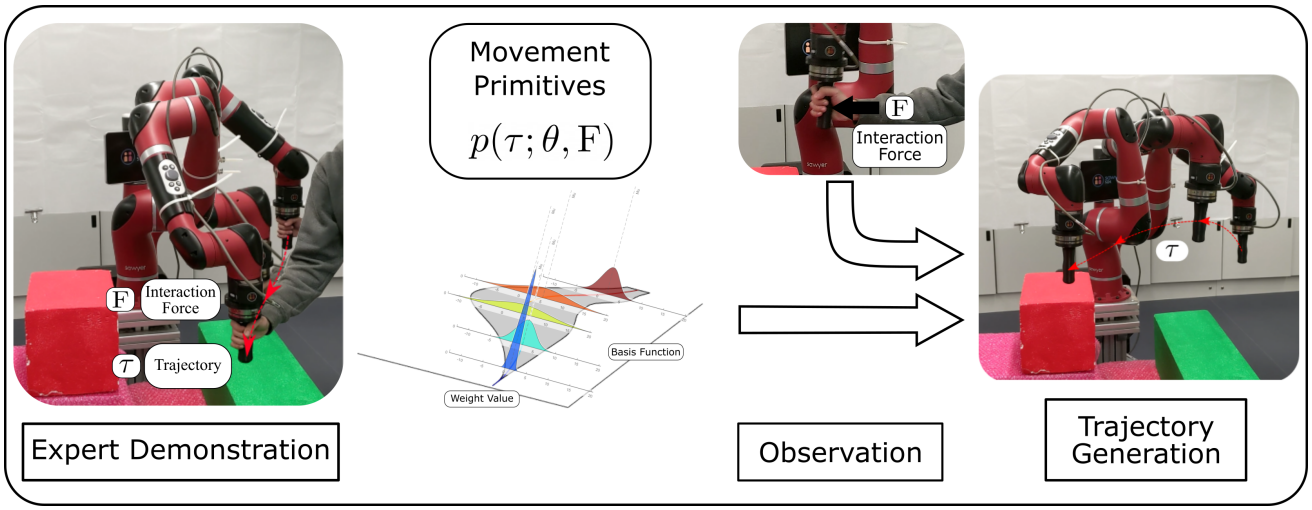

Fig. 1 Overview of Learning from Demonstration using Movement Primitives in the Bayesian context.

interactions since the user may have no prior knowledge on the dynamics of the system.

Intuitively, humans exert forces to indicate their intention during physical interactions in everyday situations such as target-reaching tasks. Thus, the integration of interaction forces in MPs may improve the estimation of user intent when generating the appropriate robotic response. More importantly, a correct intent estimate in pHRI applications contributes towards the efficacy of the robotic response. Furthermore, probabilistic models of the interaction artifacts can capture system noise and user variability simultaneously.

This article introduces physical Human Robot Interaction Primitives (pHRIP), utilizing interaction forces in a probabilistic distribution over Dynamic Movement Primitive parameters. Robotic motion parameters are inferred, conditioning upon partial observations of interaction forces representing the user's intention. The proposed method is validated through: (a) a target-directed reaching experiments; and (b) a planar and 3 Degree of Freedom (DoF) obstacle avoidance task.

This article is organized as follows: Section 2 consists of a review of related works, followed by the methodology for pHRIP in Section 3. The setup for the validation experiments are presented in Section 4, with their respective results discussed in Section 5. Finally, Section 6 discusses future work before conclude the article.

2 Review of Related Works

Movement Primitives (MP) are a family of *elementary operations* to represent robotic trajectories for motion planning. Inspired by human locomotion [23], MPs are compact representations of complex locomotion in multi-degree of freedom (DoF) systems, forming the basis for various robotic capabilities: e.g. learning, imitation, and generalization of trajectories.

One popular MP used in the robotics community is Dynamic Movement Primitives (DMP), which capture acceleration-based dynamics using low dimensional basis functions. DMP leverages expert demonstrations to model the motion using a few parameters, with favorable properties such as trajectory dilation, rotational invariance, and temporal scaling [26].

Adaptation of the original formulation to overcome limitations [21] have made DMPs suitable for many domestic and industrial applications: e.g. obstacle avoidance [18], industrial assembly [27], surface wiping [17], collaborative object transfer [42, 47], and co-operative sawing [41]. While there are adaptations or new formulations of MP such as Kernelized Movement Primitives [25] (for further compression of trajectory representation), Interactive DMPs [29] (for reaching equilibrium trajectories based on interaction forces), and Coupling Movement Primitives [16] (for achieving equal interaction forces), traditional DMPs remain popular due to their versatility and track record.

Given that there is inherent variability in human locomotion [48], applications for HRI and pHRI require some form of generalization which capture system noise and covariances across the different DoFs. This is especially crucial in multi-DoF systems for both the human and the robot, leading to applications with probabilistic models over DMP parameters, e.g. generating movement in a musculoskeletal system [44], table tennis swinging [34], and stiffness sensitive tasks [13, 36].

Due to the robustness of probabilistic models, there is a significant amount of interest in probabilistic approaches to LfD and PbD, allowing for context-driven

responses based on MPs [10,33,37]. Probabilistic modeling also paved the way for multi-model and multi-modal applications with a single model such as dust sweeping [40], teleoperation [39, 50], domestic feeding [6], industrial assembly [30], and ball throwing [51].

A probabilistic approach to trajectory generation and user intent estimation are popular due to probabilistic properties of the model, with notable applications for HRI utilizing Interaction Primitives (IP) and its extensions: e.g. human robot gestures [3], collaborative object covering [11], and hand shaking [7]. The probabilistic model embeds the user intent in their outputs, making it suitable to utilize probabilistic operators to adapt the model for goal and trajectory adaptation [2, 28, 28], sequential intent estimation [35], and stiffness adaptation [43].

While MP-based frameworks such as Coupled Cooperative Primitives [24] have been applied to exoskeletons to minimize interaction forces between the user and exoskeleton, tightly coupled systems remain a challenge for MPs in pHRI applications. Rather than the robot system initiating the task process, Compliant Parametric Dynamic Movement Primitives [49] actively incorporate user input by adapting stiffness based on the variance of the trajectory at that phase. However, such reliance on the human user to take over control might not be suitable for certain applications such as post-injury assistive robotics.

Applications of MPs in pHRI have generally relied on the modification of DMP formulations to embed interaction forces when motion planning for the robot arm. Despite the appeal for bespoke MP formulations, probabilistic approaches for MPs (without any modifications) provide robust solutions for a larger range of pHRI applications. Probabilistic operators also provide flexibility for concatenation and pruning of different objectives and observations. In the context of this work, the integration of interaction forces leverages probabilistic operators when building the model.

3 Methodology

3.1 Dynamic Movement Primitives

Dynamic Movement Primitives (DMP) generate globally stable trajectories by treating the trajectory as a spring-damper system with an attractor system to encode non-linear dynamics [45]. The attractor landscape is represented by a linear system of basis functions across time or phase.

While the original DMP formulation produced stable trajectories, a modified formulation overcame several undesired artifacts during edge case reproductions such as trajectory "mirroring" and accelerations that are beyond the capabilities of existing robots [38]. Each degree of freedom in the system is modeled as

$$\begin{aligned} \tau\dot{v} &= K(g-x) - Dv - sK(g-x_0) + sKf(s), \\ \tau\dot{x} &= v. \end{aligned} \tag{1}$$

The phase of the trajectory, s is modeled as a first-order system with parameter α for temporal scaling $\tau\dot{s} = -\alpha s$. The attractor landscape, represented by the forcing function, f, is encoded using the weighted sum of Gaussian basis functions with centers, $\boldsymbol{c}$ and is spread evenly across the phase of the trajectory

$$\begin{aligned} f(s) &= \frac{\sum_{i=1}^{M} \psi_i(s)\omega_i s}{\sum_{i=1}^{M} \psi_i(s)} = \phi(s)^T\boldsymbol{\omega}, \\ \psi_i(s) &= \exp(-(s-c_i)^2/h), \end{aligned} \tag{2}$$

producing a $M \times 1$ vector of weights, $\boldsymbol{\omega}$ for each DoF of the trajectory. While the Gaussian kernel has been used in DMPs, any smooth functions or mollifiers could alternatively be used.

Representing the forcing function (from T observations) as a linear system allows the weights to be obtained using linear least squares regression

$$\boldsymbol{f} = \begin{bmatrix} f(s_1) \\ f(s_2) \\ \vdots \\ f(s_T) \end{bmatrix} = \begin{bmatrix} \phi_1(s_1) & \dots & \phi_M(s_1) \\ \phi_1(s_2) & \dots & \phi_M(s_2) \\ \vdots & \ddots & \vdots \\ \phi_1(s_T) & \dots & \phi_M(s_T) \end{bmatrix} \begin{bmatrix} \omega_1 \\ \omega_2 \\ \vdots \\ \omega_M \end{bmatrix}, \tag{3}$$

$$\boldsymbol{\omega} = (\boldsymbol{\phi}^T\boldsymbol{\phi})^{-1}\boldsymbol{\phi}^T\boldsymbol{f}. \tag{4}$$

3.2 Physical Human Robot Interaction Primitives

Similar to most probabilistic approaches to generalize MPs, physical Human Robot Interaction Primitives (pHRIP) builds a distribution, $p(\theta)$, of both DMP parameters, capturing the demonstrated trajectories, and interaction forces. A predictive distribution is then obtained using partial observations of interaction forces between the user and robot, χ^*.

Similar to DMPs, the velocities of the interaction forces are decoupled using a monotonic function phase variable $z = [1, 2, \dots, 100]^T$. The observations of a single dimension interaction force gives a $T \times 1$ matrix $\boldsymbol{F}_{1:T} = [F_1, F_2, \dots, F_T]^T$. The interaction forces are resampled into a 100×1 matrix, $\boldsymbol{F}^*$ correlating with the z where $F_1^* = F(z_1), \dots, F_{100}^* = F(z_{100})$.

For a n-DoF robotic system and d-DoF interaction forces, the pHRIP parameter set for a single trajectory is defined as

$$\theta = [\boldsymbol{F}_1^{*T}, \dots, \boldsymbol{F}_d^{*T}, \boldsymbol{\omega}_1{}^T, \dots, \boldsymbol{\omega}_n{}^T], \tag{5}$$

and the distribution of the pHRIP parameters $p(\theta)$ for K trajectories follows as

$$p(\theta) = \mathcal{N}(\theta|\mu_\theta, \Sigma_\theta), \tag{6}$$

$$\mu_\theta = \frac{\sum_{j=1}^{K} \theta_j}{K}, \tag{7}$$

$$\Sigma_\theta = \frac{\sum_{j=1}^{K} (\theta_j - \mu_\theta)^T (\theta_j - \mu_\theta)}{K}. \tag{8}$$

The partial observations of interaction forces is phase-aligned using a multi-dimensional Dynamic Time Warping (DTW) algorithm [46]. Given one set of t partial observations, $\chi^*_{1:t} = [x^*_1, x^*_2, \ldots, x^*_t]$, DTW measures the similarity between the partial observations to a reference trajectory, $\chi_{1:T} = [x_1, x_2, \ldots, x_T]$. The resultant integer phase indices, $\boldsymbol{\rho} = [\rho_1, \rho_2, \ldots, \rho_t]$ for the partial observations reflect the frame in the reference movement which produces a minimum distance between the two time series,
i.e. $D = [min(\chi^*_1, \chi_{\rho_1}), min(\chi^*_2, \chi_{\rho_2}), \ldots, min(\chi^*_t, \chi_{\rho_t})]$.

The predictive distribution of the parameters is obtained using partial observations, χ^*, between the user and the robot and applying Bayes rule:
e.g. $p(\theta|\chi^*) \propto p(\chi^*|\theta)p(\theta)$.

The partial observations consists of the interaction forces, $\chi^* = [F^{**}, \tau_r]$, where the unavailable trajectories of the robot, τ_r, are set to 0.

Modeling the likelihood distribution, $p(\chi^*|\theta)$ is done using a Gaussian distribution over the phase indices from the partial observations of the interaction forces

$$p(\chi^*|\theta) \sim \mathcal{N}(\chi^*|\Omega\theta, \sigma^2 I), \tag{9}$$

$$\Omega\theta = \begin{bmatrix} \phi_1 & 0 & \ldots\ldots & 0 \\ 0 & \ddots & \ddots & \vdots \\ \vdots & \ddots & \phi_d & \ddots \\ \vdots & \ddots & \ddots & \vdots \\ 0 & \ldots\ldots & & 0 \end{bmatrix} \begin{bmatrix} z_1 \\ \vdots \\ z_d \\ \omega_1 \\ \vdots \\ \omega_n \end{bmatrix}. \tag{10}$$

where σ^2 is the observation variance. ϕ relates the interaction forces to the phase indices from DTW of partial observations with t samples. With ϕ_{11} referring to the matrix element in row 1 and column 1, ϕ is a $t \times 100$ matrix with elements defined as

$$\phi_{xy} = \begin{cases} 1 & for\ y = \rho_x \\ 0 & for\ y \neq \rho_x \end{cases}, where \\ x \in (1, 2, \ldots, t), \\ y \in (1, 2, \ldots, 100). \tag{11}$$

Given the likelihood $p(\chi^*|\theta)$, the joint distribution is defined as

$$p(\chi^*, \theta) = \mathcal{N}\left(\begin{bmatrix} \chi^* \\ \theta \end{bmatrix} \middle| \begin{bmatrix} \omega\theta \\ \mu_\theta \end{bmatrix}, \begin{bmatrix} A & \Sigma_\theta \Omega^T \\ \Omega\Sigma_\theta & \Sigma_\theta \end{bmatrix} \right), \tag{12}$$

where $A = \sigma^2 I + \Omega\Sigma_\theta\Omega^T$, and the mean and variance of conditional distribution, $p(\theta|\chi^*)$ is derived as

$$\mu_{\theta|\chi^*} = \mu_\theta + \Sigma_\theta \Omega^T A^{-1}(\chi^* - \Omega\mu_\theta), \\ \Sigma_{\theta|\chi^*} = \Sigma_\theta - \Sigma_\theta \Omega^T A^{-1} \Omega \Sigma_\theta. \tag{13}$$

A new set of pHRIP parameters, θ is then sampled from this conditional distribution and the robot is operated with the new DMP weights and the estimated phase of the final observation, ρ_t.

4 Implementation and Evaluation

A series of validation experiments and trials were conducted to validate pHRIP in a coupled system, an arrangement commonly seen in pHRI applications. The setup of the coupled system is shown in Figure 2 and consists of a 7 DoF Sawyer robotic manipulator (HAHN Robotics, Germany) with a 6-axis Axia80 force-torque sensor (ATI Industrial Automation, USA) affixed between the end effector and a bespoke handle. Robotic data from the Sawyer robotic manipulator are recorded at 100Hz while wrench data from the force-torque sensor is recorded at 125Hz.

In all experiments and trials, the robotic arm utilizes Rethink Robotics' proprietary software, Intera SDK, and an end effector velocity threshold of $2.5cms^{-1}$ is used to determine the start and end of the demonstration. In all experiments, generated trajectories were

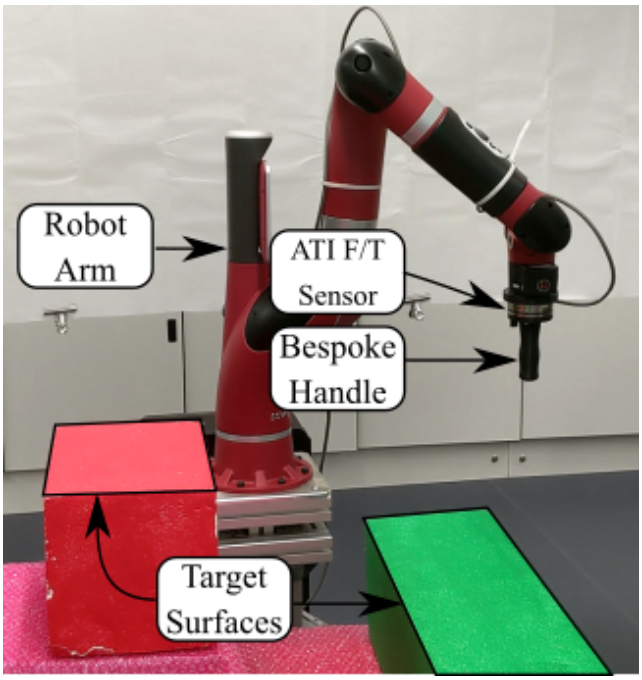

Fig. 2 The experimental setup with a Sawyer robot arm, an ATI Axia80 force-torque (F/T) sensor, and a bespoke handle.

sent to the robot's native motion controller interface to be performed in an open-loop fashion. While it is possible to integrate low-level robotic feedback controllers with pHRIP, this article focuses on the trajectory generation process which reflects the user's intention.

4.1 Human Target Reaching Experiments

An experiment based on target-directed movements was conducted to validate pHRIP's robustness to different users. Four participants (3 male and 1 female) took part in the experiment. During user interactions, the robotic arm was setup to enter an orientation-locked zero-g mode.

Participants were instructed to move the handle from a defined starting position to one of two target surfaces (Figure 2) in a "natural manner". Each trial consists of a reference and a test trajectory, with participants instructed to perform both trajectories "consistently".

A total of 90 training demonstrations were recorded (45 for each target surface) using kinesthetic teaching via the bespoke handle for participants. During the test trajectory, participants were instructed to release the handle after 0.5-1.0 seconds while the new trajectory is generated and performed by the robot arm.

Partial observations for DMP consist of Cartesian trajectory while pHRIP utilized Cartesian interaction forces only. Partial observations of both interaction forces and trajectory were used to perform further comparisons. Prior to the start of the experiment, participants were given a 5-minute window to interact with the robotic manipulator to familiarize themselves with the setup.

4.2 Planar Obstacle Avoidance

A planar obstacle avoidance experiment was conducted to validate pHRIP and compare against DMP, with the setup shown in Figure 3. A total of 30 training trajectories and 20 testing trajectories were recorded while the robotic arm is setup to enter an orientation-locked zero-g mode constrained to the XY plane.

The analysis and trajectory generation for the planar obstacle avoidance experiment were conducted post-hoc. Thus, all recorded trajectories and interaction forces were re-sampled to 400 and 500 samples respectively. A comparison between DMP and pHRIP is performed using partial observations of: (a) trajectory only (DMP); and (b) interaction force only (pHRIP).

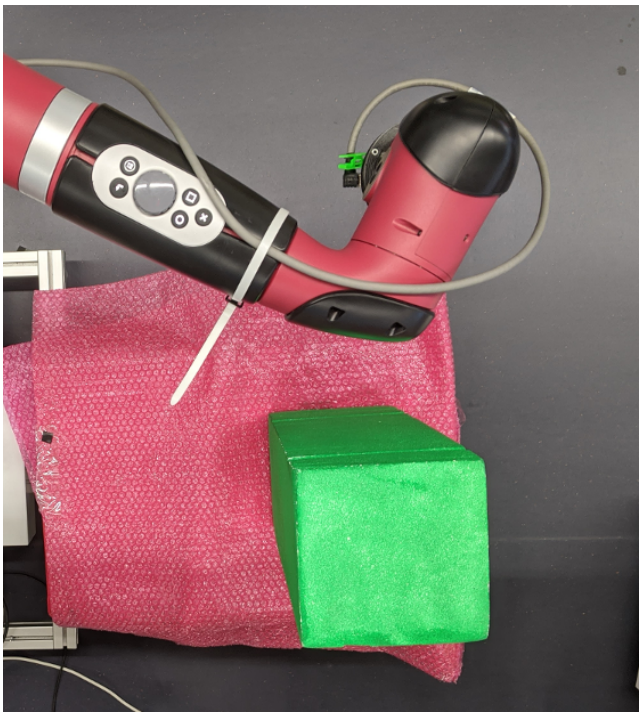

Fig. 3 A top-down view of the planar validation setup.

4.3 Cartesian Obstacle Avoidance

Further experiments were conducted to reinforce the applicability of pHRIP to estimate user intention during pHRI. The user is tasked with moving the end effector from the same starting position to various end regions. A series of obstacles were set up in varying configurations which simulate changing environments and task parameters, as is common in pHRI applications.

Using a number of identical obstacle blocks, each setup was configured such that multiple valid approaches to reach the end region were available. For each setup, the user recorded 10 training trajectories with identical approaches during obstacle avoidance to reach the end region. The four workspace configurations for this experiment are shown in Figure 4.

A series of trials were conducted in which the obstacle configurations were randomly chosen. Similar to the target reaching task, the user released the handle after 0.5-1.0s, allowing the robot to perform the trajectory generated by pHRIP. For each trial to be labeled successful, the robot arm (including external wires from peripheral systems) must not come in contact with any obstacles and reach the desired end region.

One issue which arises when the number of samples for each trajectory are different in DMP is the sum of activation from the basis functions. A static value of τ will affect the quality of the reproduced trajectory based on the sample length. Assuming that the other

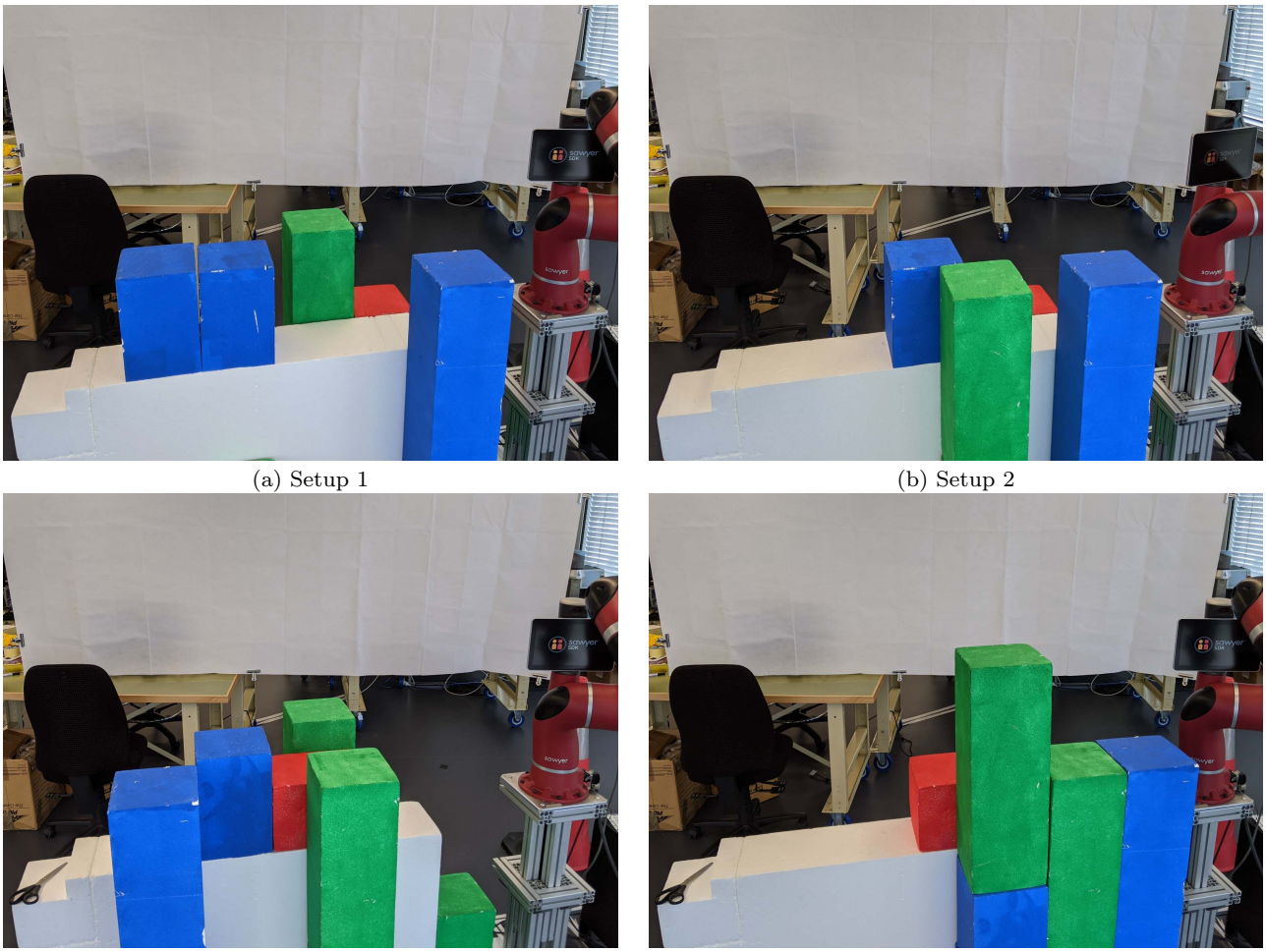

(a) Setup 1 (b) Setup 2

(c) Setup 3 (d) Setup 4

Fig. 4 The four workspace configurations used for training in the Cartesian obstacle avoidance experiment.

DMP parameters are constant, an exponential model can be used to determine the relationship between the trajectory length (number of samples λ) and a τ value which ensures that the sum of Gaussian basis function activation across all samples are above 0.5. For all trials in the Cartesian obstacle avoidance experiment, the model and its coefficients used are

$$\begin{aligned} &\tau = a \cdot exp(b * \lambda) + c \cdot exp(d * \lambda) \\ &a = 2.22 \qquad\qquad b = -0.01292 \\ &c = 0.4684 \qquad\qquad d = -0.001595 \end{aligned} \tag{14}$$

Other than the four configurations used for training trajectories, a novel configuration (see Figure 12) was used to test the robustness of pHRIP when generating trajectories to infer user intent to avoid obstacles.

5 Results and Discussion

5.1 Human Target Reaching Experiment

A total of 28 trials were conducted in the experiment. For each trial, participants demonstrated a reference trajectory as shown in Figure 5(a). Partial observations were then used to generate new trajectories. Trajectories were generated post-hoc using DMP and pHRIP. Partial observations of trajectories were used for DMP and the resultant output shown in Figure 5(b). For pHRIP, partial observations of interaction forces were used with the resultant outputs shown in Figure 5(c).

Visual inspection of the trajectories between DMP and pHRIP indicates the advantage of pHRIP over DMP. Using only interaction forces, the trajectories generated from pHRIP followed the shape of those in the reference trajectories. This is evident in the DTW scores in Table 1 of the generated trajectories indicating a better match in shape to the reference trajectory.

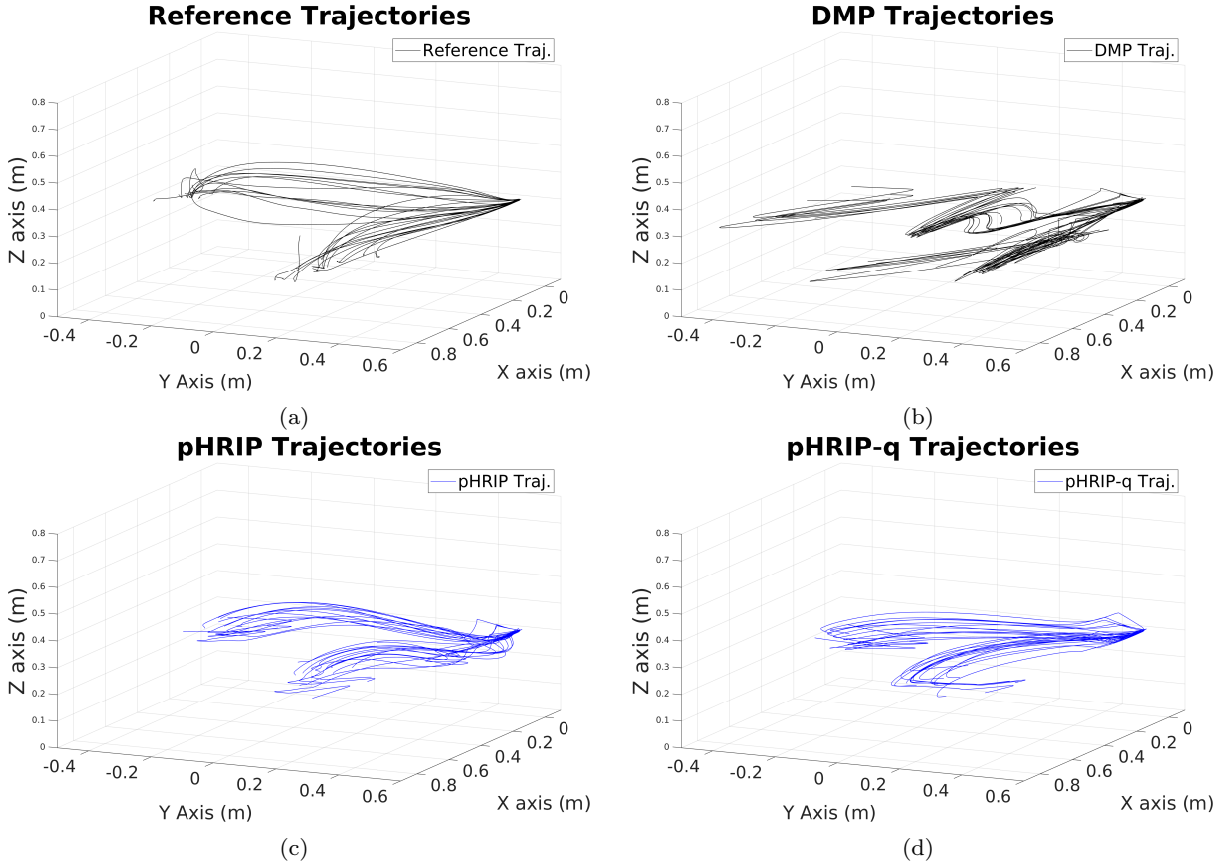

Fig. 5 The trajectories from the human 3-DoF experiment trials. (a) Reference trajectories from participants. Trajectories generated from: (b) trajectory observations using DMP; (c) interaction forces using pHRIP; and (d) interaction forces using pHRIP-q in joint state space.

The effect of the observation length between trajectories generated using DMP and pHRIP can be seen in Figure 7, indicating the DTW distances for trajectories generated using pHRIP are much lower than those of DMP. As observation lengths increase, errors from the generated trajectories would approach zero, giving diminishing returns for pHRIP or DMP. While a longer observation can improve the performance of HRI applications using movement primitives, this is undesirable in pHRI applications since the goal of the robot is to contribute meaningfully as soon as possible. Trajectories from pHRIP consistently produce better trajectories when compared against DMP, reinforcing our hypothesis that using interaction forces during pHRI can help reduce uncertainty.

5.2 Cartesian vs. Joint State Trajectory

While pHRIP has been shown to generate trajectories that reflect the user's intention in Cartesian space, for most robotic arm control systems, action policies generally operate in joint space. Further analysis was conducted post-hoc using the data from the human target reaching experiment to investigate the application of pHRIP in joint state space (pHRIP-q). The joint states of the robot and the Cartesian interaction forces at the end effector were used to build the weight distribution.

Table 1 A comparison of the RMSE and DTW distance between trajectories generated from DMP, pHRIP, and pHRIP-q. The same reference trajectory was used for each trial during the analysis. The mean, μ and variance, σ^2 of the two metrics are tabulated here.

	DMP		pHRIP				pHRIP-q			
			Force Only		Force & Trajectory		Force Only		Force & Trajectory	
	μ	σ^2	μ	σ^2	μ	σ^2	μ	σ^2	μ	σ^2
RMSE (m)	0.2657	0.0031	0.1597	0.0030	0.1737	0.0024	0.1191	0.0049	0.1191	0.0049
DTW	4.2664	0.9732	1.6874	0.3056	1.8682	0.3800	1.6271	0.5728	1.6271	0.5725

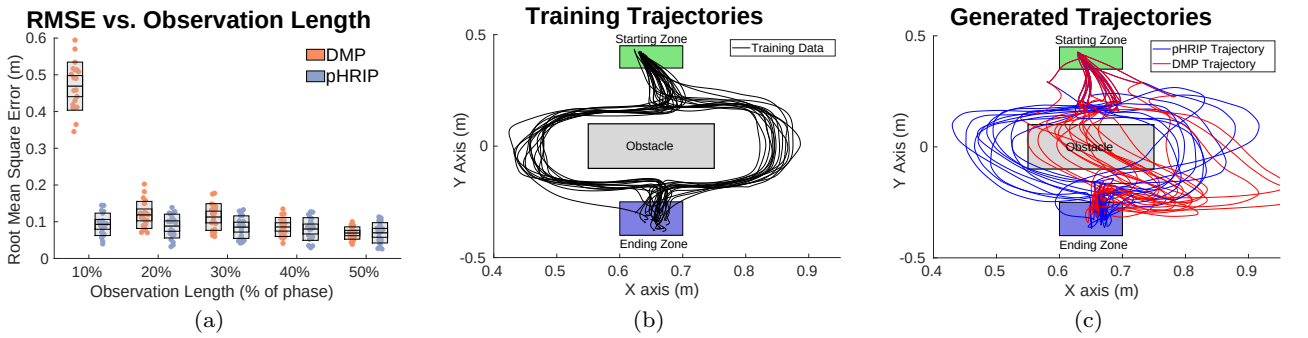

Fig. 6 The results from the planar obstacle avoidance task. (a) This highlights the RMSE spread between pHRIP and DMP for 20 observations across varying observation lengths; (b) displays the training trajectories recorded to avoid the obstacle; and (c) shows the trajectories generated by pHRIP and DMP when 30% of the trajectory is observed.

Forward kinematics was performed using the generated joint trajectories to obtain the Cartesian trajectories.

For both the original human target reaching experiment and this analysis, identical parameters were used with 20 basis functions, $K = 80N/m$, $D = 20Ns/m$, $\tau = 0.35$, $h = 0.0008$, and $\alpha = 1$. Forward kinematics was performed for the pHRIP-q trajectories to obtain their Cartesian trajectories, showing similar trajectory shapes to the reference trajectories (see Figure 5(d)). This is supported by the mean RMSE and DTW distances as tabulated in Table 1.

Initial observations of the overall results suggest that pHRIP-q is the better variant. However, mapping out the vectorized difference between the reference and resultant endpoint, as seen in Figure 8, suggest that the appropriate pHRIP variant will depend on the priority of the task. For example, pick and place operations of heavy objects will prioritise the precise endpoint of the trajectory, making pHRIP more appropriate. Conversely, if the task is to conform to the shape of a trajectory performed by an expert, as is commonly seen during physical rehabilitation, it may be more suitable to use the joint variant of pHRIP.

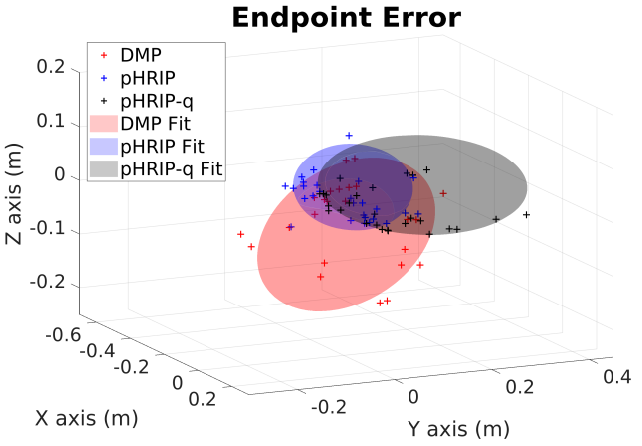

Fig. 8 A visualization of the discrepancy between the endpoint in the reference trajectories and those generated from DMP, pHRIP, and pHRIP-q. Ellipsoid fitting indicating the spread is performed using [32].

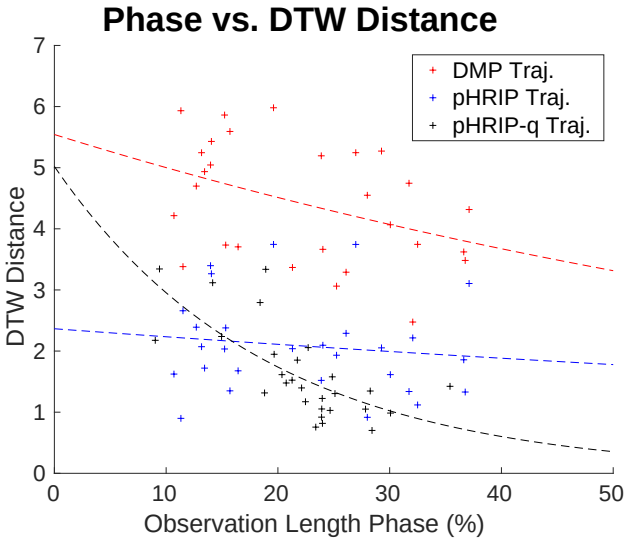

Fig. 7 The relationship between observation lengths and DTW distances when generating trajectories using DMP, pHRIP, and pHRIP-q.

While the results show that appropriate consideration is required when choosing which variant to use, they show promising indications for the integration of haptic information during motor skill learning in pHRI applications. One potential for pHRI application is in training and development systems, where expert demonstrations may be collected remotely via a haptic interface, providing intuitive motor skill learning remotely. Learning from the interaction forces on the haptic interface is transferable across various platforms provided kinesthetic teaching of the robotic response is performed.

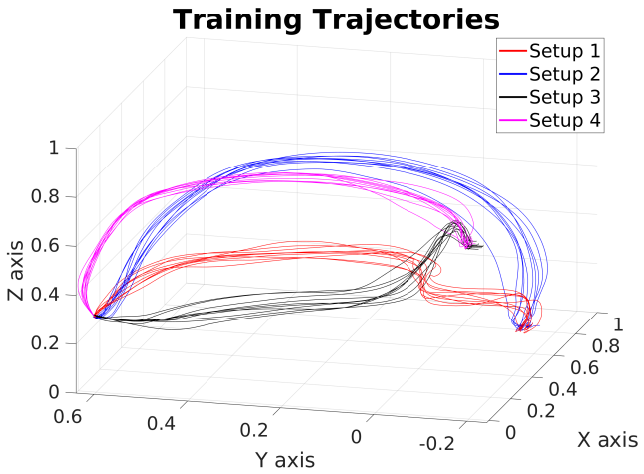

Fig. 9 The training trajectories for the Cartesian obstacle avoidance task.

5.3 Planar Obstacle Avoidance

For the 20 test trials conducted in the planar validation, the RMSE between the generated trajectories and their respective reference trajectories was calculated. The pHRIP and DMP tests were conducted post-hoc against observation lengths (as a % of the total trajectory) varying from 10% to 50%.

Results shown in Figure 6(a) highlight the ability for pHRIP to address ambiguities in the trajectories, utilizing only interaction forces to generate the intended path. The critical advantage of pHRIP over DMPs is shown when there are less observations such as those when only 10% of the trajectory is observed.

While the results may indicate that the advantage of pHRIP diminishes as more observations are obtained, the generated trajectories highlight an aspect of motor skill learning which is not inherited through DMPs. The task to avoid the static obstacle is redundant, meaning there are multiple ways to complete the task. During the recording of training trajectories, two distinct paths were taught kinesthetically by the demonstrator, showing this phenomenon as seen in Figure 6(b). From Figure 6(c), trajectories generated by DMP (in red) all collide with the obstacle severely while the same only occur to 25% of pHRIP trajectories. Observations of the pHRIP trajectories also show decreased severity during collisions, with only two trajectories (10%) clearly going through the obstacle.

The results in Figure 6(c) highlight the limitation of DMPs in multi-modal distributions which is overcome by using the interaction forces in pHRIP. This reinforces our belief that the integration of interaction artifacts improve motor skill learning for pHRI systems and provide a better inference of user intention.

Table 2 Measures of similarity against the user's reference trajectory indicating their intention.

	DTW Distance (unitless)		RMSE (m)
	μ	σ^2	μ
Successful	2.3482	0.2704	0.1697
Unsuccessful	3.3793	0.8941	0.2202

5.4 Cartesian Obstacle Avoidance

For the 4 configuration setup, 10 training trajectories were recorded each and are shown in Figure 9. In total, 12 trials were conducted to validate pHRIP in an

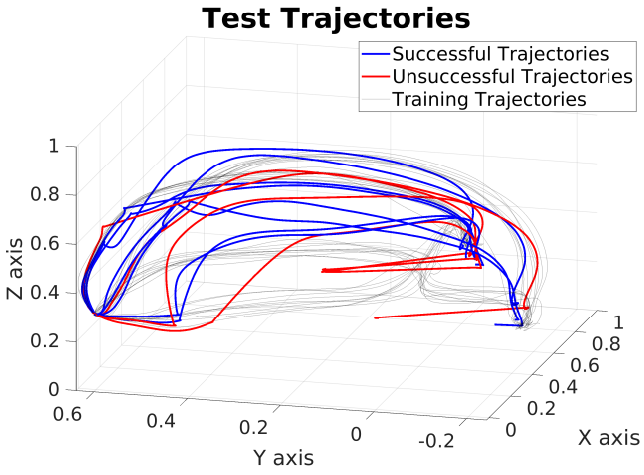

Fig. 10 The trajectories from the experiment. Trials that reached the intended target and did not hit any obstacles are shown in blue while unsuccessful paths are shown in red.

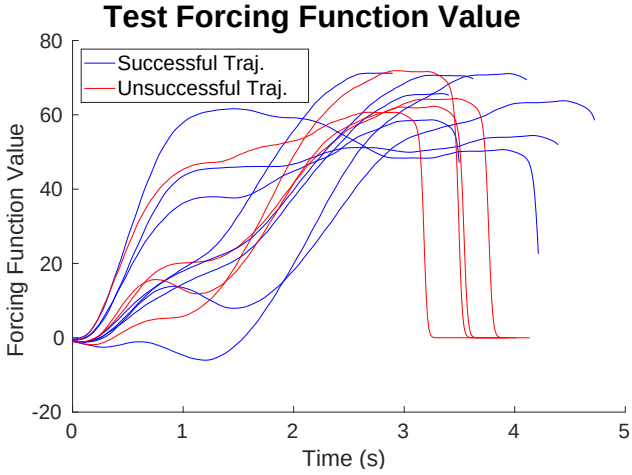

Fig. 11 The forcing function values for the experiment trials. Successful trajectories are shown in blue while unsuccessful trajectories are shown in red.

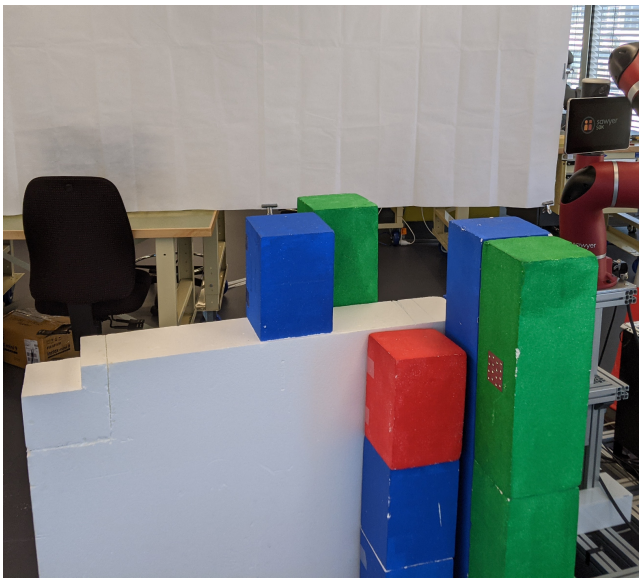

Fig. 12 Novel configuration setup for testing pHRIP's adaptation capabilities.

obstacle avoidance task in Cartesian space. Successful trials are defined as generated trajectories that reach their intended end zone while not touching any obstacles along the way. For all trials, identical sets of parameters were used with 30 basis functions, $K = 80N/m$, $D = 20Ns/m$, $h = 0.0008$, and $\alpha = 0.8$. For each trial, an estimate of τ parameter is performed using the reference trajectory length.

Of the 12 trials, there were 4 unsuccessful trajectories which all hit obstacles towards the end of the trajectory as seen in Figure 10. Visual observations of the trajectories show that unsuccessful trajectories were caused by inaccurate estimates of the τ parameter. This phenomenon is evident in Figure 11 where the forcing function value for the unsuccessful trajectories drops to 0, causing the trajectories to deviate significantly. For the successful trials, pHRIP was able to correctly infer the user's intent when generating trajectories to avoid the obstacles.

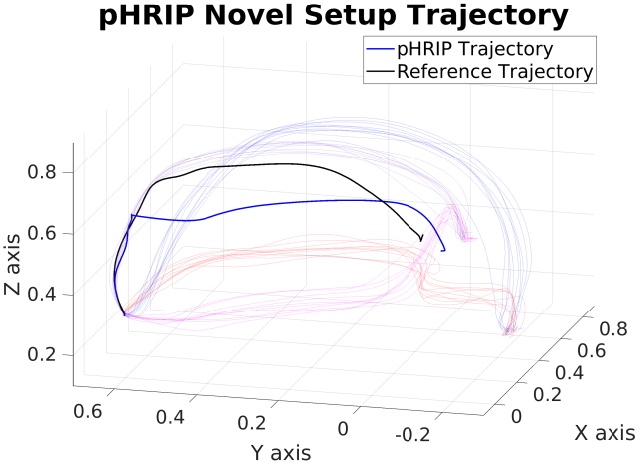

Fig. 13 The trajectory generated for the novel setup and the reference trajectory.

To test the adaptability of pHRIP, a novel setup was designed as shown in Figure 12. New weights are conditioned over the distribution built on the same set of training trajectories[1]. The trajectory generated from pHRIP was able to match the shape of the user intent while avoiding obstacles and end within 10cm of the new end zone.

6 Conclusion and Future Work

This article introduces physical Human Robot Interaction Primitives (pHRIP), a framework that can infer the user's intention to generate the appropriate robotic response during physical human robot interactions using only the interaction forces. pHRIP extends upon DMPs by embedding interaction forces in the distribution over the robotic response to allow for user intent inference when generating robotic trajectories.

A series of experiments based on target-directed reaching and obstacle avoidance tasks were conducted to validate the efficacy of pHRIP, showing accurate inference of user intent with a small number of observations. Comparisons of a planar obstacle avoidance task demonstrated the advantage of utilizing interaction forces in pHRIP, instead of the robot trajectory in DMPs, during multi-modal tasks for pHRI. The adaptation of pHRIP to novel situations also demonstrates its robustness, with possibilities to integrate with multi-model probabilistic techniques in the future.

While the experiments to validate pHRIP are approached through the lense of motion planning to reflect user intent, developing a control system which derives from pHRIP outputs will create opportunities to improve user assistance during pHRI. Furthermore, the utilization of interaction forces has highlighted the need to explore the variability exhibited by humans during pHRI to provide a personalized experience.

In the context of human biomechanics, the interaction forces during pHRI can be derived from external systems decoupled from the robotic platform such as biomechanical models [44] and physiological measures [41]. Thus, future work will explore the effects of context-dependent observations for pHRIP, leveraging knowledge on the non-linear behavior of human locomotion and force generation [12, 22].

[1] Video for the experiment can be found at https://youtu.be/idKgVGCuMw0

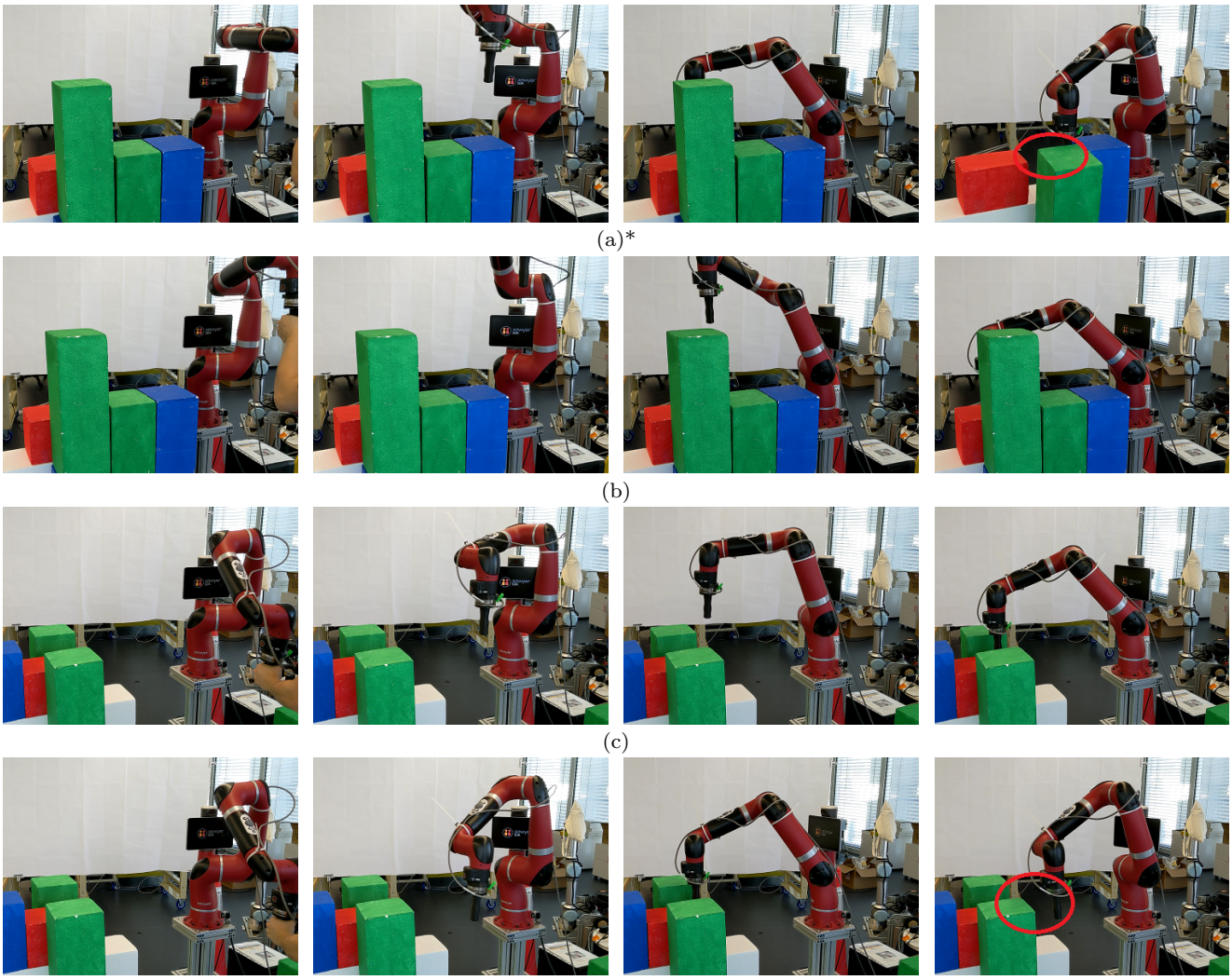

Fig. 14 The behavior of pHRIP for known setups. * indicates an unsuccessful trial with the red ellipse showing the collisions.

Acknowledgements The authors would like to thank Jaime Valls Miros for his insightful comments and feedback about the article. The authors would also like to thank Marc Carmichael for his discussions about the article.

This research is supported by an Australian Government Research Training Program scholarship and a UTS FEIT HDR Collaboration Experience Award.

References

1. Argall, B.D., Chernova, S., Veloso, M., Browning, B.: A survey of robot learning from demonstration. Robotics and Autonomous Systems **57**(5), 469–483 (2009). DOI 10.1016/j.robot.2008.10.024
2. Bajcsy, A., Losey, D.P., O'malley, M.K., Dragan, A.D.: Learning Robot Objectives from Physical Human Interaction. Proceedings of Machine Learning Research **78**, 217–226 (2017)
3. Ben Amor, H., Neumann, G., Kamthe, S., Kroemer, O., Peters, J.: Interaction primitives for human-robot cooperation tasks. In: Proceedings - IEEE International Conference on Robotics and Automation, pp. 2831–2837. Institute of Electrical and Electronics Engineers Inc. (2014). DOI 10.1109/ICRA.2014.6907265
4. Billard, A., Calinon, S., Dillmann, R., Schaal, S.: Robot Programming by Demonstration. In: B. Siciliano, O. Khatib (eds.) Springer Handbook of Robotics, pp. 1371–1394. Springer Berlin Heidelberg, Berlin, Heidelberg (2008). DOI 10.1007/978-3-540-30301-5{_}60
5. Bloss, R.: Collaborative robots are rapidly providing major improvements in productivity, safety, programing ease, portability and cost while addressing many new applications. Industrial Robot **43**(5), 463–468 (2016). DOI 10.1108/IR-05-2016-0148
6. Calinon, S., D'Halluin, F., Sauser, E.L., Caldwell, D.G., Billard, A.G.: Learning and reproduction of gestures by imitation. IEEE Robotics and Automation Magazine **17**(2), 44–54 (2010). DOI 10.1109/MRA.2010.936947
7. Campbell, J., Stepputtis, S., Ben Amor, H.: Probabilistic Multimodal Modeling for Human-Robot Interaction Tasks. In: Proceedings of Robotics: Science and Systems. FreiburgimBreisgau, Germany (2019). DOI 10.15607/RSS.2019.XV.047

8. Carmichael, M.G., Aldini, S., Khonasty, R., Tran, A., Reeks, C., Liu, D., Waldron, K.J., Dissanayake, G.: The ANBOT: An Intelligent Robotic Co-worker for Industrial Abrasive Blasting. In: 2019 IEEE/RSJ International Conference on Intelligent Robots and Systems (IROS), pp. 8026–8033. Institute of Electrical and Electronics Engineers (IEEE), Macau, China (2019). DOI 10.1109/iros40897.2019.8967993
9. Carmichael, M.G., Liu, D., Waldron, K.J.: A framework for singularity-robust manipulator control during physical human-robot interaction. The International Journal of Robotics Research **36**(5-7), 861–876 (2017). DOI 10.1177/0278364917698748
10. Cui, Y., Poon, J., Matsubara, T., Miro, J.V., Sugimoto, K., Yamazaki, K.: Environment-adaptive interaction primitives for human-robot motor skill learning. In: IEEE-RAS International Conference on Humanoid Robots, pp. 711–717. IEEE Computer Society (2016). DOI 10.1109/HUMANOIDS.2016.7803352
11. Cui, Y., Poon, J., Miro, J.V., Yamazaki, K., Sugimoto, K., Matsubara, T.: Environment-adaptive interaction primitives through visual context for human–robot motor skill learning. Autonomous Robots **43**(5), 1225–1240 (2019). DOI 10.1007/s10514-018-9798-2
12. D'Avella, A., Saltiel, P., Bizzi, E.: Combinations of muscle synergies in the construction of a natural motor behavior. Nature Neuroscience **6**(3), 300–308 (2003). DOI 10.1038/nn1010
13. Denisa, M., Gams, A., Ude, A., Petric, T.: Learning Compliant Movement Primitives Through Demonstration and Statistical Generalization. IEEE/ASME Transactions on Mechatronics **21**(5), 2581–2594 (2016). DOI 10.1109/TMECH.2015.2510165
14. Djuric, A.M., Urbanic, R.J., Rickli, J.L.: A Framework for Collaborative Robot (CoBot) Integration in Advanced Manufacturing Systems. SAE International Journal of Materials and Manufacturing **9**(2), 457–464 (2016). URL `https://www.jstor.org/stable/26267460`
15. Ferraguti, F., Talignani Landi, C., Sabattini, L., Bonfè, M., Fantuzzi, C., Secchi, C.: A variable admittance control strategy for stable physical human–robot interaction. The International Journal of Robotics Research **38**(6), 747–765 (2019). DOI 10.1177/0278364919840415
16. Gams, A., Nemec, B., Ijspeert, A.J., Ude, A.: Coupling movement primitives: Interaction with the environment and bimanual tasks. IEEE Transactions on Robotics **30**(4), 816–830 (2014). DOI 10.1109/TRO.2014.2304775
17. Gams, A., Petrič, T., Do, M., Nemec, B., Morimoto, J., Asfour, T., Ude, A.: Adaptation and coaching of periodic motion primitives through physical and visual interaction. Robotics and Autonomous Systems **75**, 340–351 (2016). DOI 10.1016/j.robot.2015.09.011
18. Ginesi, M., Meli, D., Calanca, A., Dall'Alba, D., Sansonetto, N., Fiorini, P.: Dynamic Movement Primitives: Volumetric Obstacle Avoidance. In: 2019 19th International Conference on Advanced Robotics (ICAR), pp. 234–239. Institute of Electrical and Electronics Engineers (IEEE) (2019). DOI 10.1109/icar46387.2019.8981552
19. Haddadin, S., De Luca, A., Albu-Schäffer, A.: Robot collisions: A survey on detection, isolation, and identification. IEEE Transactions on Robotics **33**(6), 1292–1312 (2017). DOI 10.1109/TRO.2017.2723903
20. Hamaya, M., Matsubara, T., Noda, T., Teramae, T., Morimoto, J.: Learning assistive strategies for exoskeleton robots from user-robot physical interaction. Pattern Recognition Letters **99**, 67–76 (2017). DOI 10.1016/j.patrec.2017.04.007
21. Hoffmann, H., Pastor, P., Park, D.H., Schaal, S.: Biologically-inspired dynamical systems for movement generation: Automatic real-time goal adaptation and obstacle avoidance. In: 2009 IEEE International Conference on Robotics and Automation, pp. 2587–2592. Institute of Electrical and Electronics Engineers (IEEE) (2009). DOI 10.1109/robot.2009.5152423
22. Hogan, N.: The mechanics of multi-joint posture and movement control. Biological Cybernetics **52**(5), 315–331 (1985). DOI 10.1007/BF00355754
23. Hogan, N., Sternad, D.: Dynamic primitives in the control of locomotion. Frontiers in Computational Neuroscience **7**, 71 (2013). DOI 10.3389/fncom.2013.00071
24. Huang, R., Cheng, H., Qiu, J., Zhang, J.: Learning Physical Human-Robot Interaction with Coupled Cooperative Primitives for a Lower Exoskeleton. IEEE Transactions on Automation Science and Engineering **16**(4), 1566–1574 (2019). DOI 10.1109/TASE.2018.2886376
25. Huang, Y., Rozo, L., Silvério, J., Caldwell, D.G.: Kernelized movement primitives. The International Journal of Robotics Research **38**(7), 833–852 (2019). DOI 10.1177/0278364919846363
26. Ijspeert, A.J.: Central pattern generators for locomotion control in animals and robots: A review. Neural Networks **21**(4), 642–653 (2008). DOI 10.1016/j.neunet.2008.03.014
27. Karlsson, M., Carlson, F.B., Robertsson, A., Johansson, R.: Two-Degree-of-Freedom Control for Trajectory Tracking and Perturbation Recovery during Execution of Dynamical Movement Primitives. IFAC-PapersOnLine **50**(1), 1923–1930 (2017). DOI 10.1016/j.ifacol.2017.08.383
28. Koert, D., Pajarinen, J., Schotschneider, A., Trick, S., Rothkopf, C., Peters, J.: Learning Intention Aware Online Adaptation of Movement Primitives. IEEE Robotics and Automation Letters **4**(4), 3719–3726 (2019). DOI 10.1109/LRA.2019.2928760
29. Kulvicius, T., Biehl, M., Aein, M.J., Tamosiunaite, M., Wörgötter, F.: Interaction learning for dynamic movement primitives used in cooperative robotic tasks. Robotics and Autonomous Systems **61**(12), 1450–1459 (2013). DOI 10.1016/j.robot.2013.07.009
30. Kyrarini, M., Haseeb, M.A., Ristić-Durrant, D., Gräser, A.: Robot learning of industrial assembly task via human demonstrations. Autonomous Robots **43**(1), 239–257 (2019). DOI 10.1007/s10514-018-9725-6
31. Lai, Y., Sutjipto, S., Clout, M.D., Carmichael, M.G., Paul, G.: GAVRe2 : Towards Data-Driven Upper-Limb Rehabilitation with Adaptive-Feedback Gamification. In: 2018 IEEE International Conference on Robotics and Biomimetics (ROBIO), pp. 164–169. IEEE (2018). DOI 10.1109/ROBIO.2018.8665105
32. Li, Q., Griffiths, J.G.: Least squares ellipsoid specific fitting. In: Proceedings - Geometric Modeling and Processing 2004, pp. 335–340 (2004). DOI 10.1109/gmap.2004.1290055
33. Maeda, G.J., Neumann, G., Ewerton, M., Lioutikov, R., Kroemer, O., Peters, J.: Probabilistic movement primitives for coordination of multiple human–robot collaborative tasks. Autonomous Robots **41**(3), 593–612 (2017). DOI 10.1007/s10514-016-9556-2
34. Matsubara, T., Hyon, S.H., Morimoto, J.: Learning stylistic dynamic movement primitives from multiple demonstrations. In: IEEE/RSJ 2010 International Conference on Intelligent Robots and Systems, IROS 2010 - Conference Proceedings, pp. 1277–1283 (2010). DOI 10.1109/IROS.2010.5651049

35. Matsubara, T., Miro, J.V., Tanaka, D., Poon, J., Sugimoto, K.: Sequential intention estimation of a mobility aid user for intelligent navigational assistance. In: Proceedings - IEEE International Workshop on Robot and Human Interactive Communication, vol. 2015-November, pp. 444–449. Institute of Electrical and Electronics Engineers Inc. (2015). DOI 10.1109/ROMAN.2015.7333580
36. Nemec, B., Likar, N., Gams, A., Ude, A.: Human robot cooperation with compliance adaptation along the motion trajectory. Autonomous Robots **42**(5), 1023–1035 (2018). DOI 10.1007/s10514-017-9676-3
37. Paraschos, A., Daniel, C., Peters, J., Neumann, G.: Using probabilistic movement primitives in robotics. Autonomous Robots **42**(3), 529–551 (2018). DOI 10.1007/s10514-017-9648-7
38. Pastor, P., Hoffmann, H., Asfour, T., Schaal, S.: Learning and generalization of motor skills by learning from demonstration. In: IEEE International Conference on Robotics and Automation, pp. 763–768. Institute of Electrical and Electronics Engineers (IEEE) (2009). DOI 10.1109/robot.2009.5152385
39. Pervez, A., Latifee, H., Ryu, J.H., Lee, D.: Motion encoding with asynchronous trajectories of repetitive teleoperation tasks and its extension to human-agent shared teleoperation. Autonomous Robots **43**(8), 2055–2069 (2019). DOI 10.1007/s10514-019-09853-4
40. Pervez, A., Lee, D.: Learning task-parameterized dynamic movement primitives using mixture of GMMs. Intelligent Service Robotics **11**(1), 61–78 (2018). DOI 10.1007/s11370-017-0235-8
41. Peternel, L., Tsagarakis, N., Caldwell, D., Ajoudani, A.: Robot adaptation to human physical fatigue in human–robot co-manipulation. Autonomous Robots **42**(5), 1011–1021 (2018). DOI 10.1007/s10514-017-9678-1
42. Prada, M., Remazeilles, A., Koene, A., Endo, S.: Dynamic Movement Primitives for Human-Robot interaction: Comparison with human behavioral observation. In: IEEE International Conference on Intelligent Robots and Systems, pp. 1168–1175 (2013). DOI 10.1109/IROS.2013.6696498
43. Rozo, L., Calinon, S., Caldwell, D.G., Jiménez, P., Torras, C.: Learning Physical Collaborative Robot Behaviors From Human Demonstrations. IEEE Transactions on Robotics **32**(3), 513–527 (2016). DOI 10.1109/TRO.2016.2540623
44. Rückert, E., d'Avella, A.: Learned parametrized dynamic movement primitives with shared synergies for controlling robotic and musculoskeletal systems. Frontiers in Computational Neuroscience **7**(OCT), 138 (2013). DOI 10.3389/fncom.2013.00138
45. Schaal, S., Peters, J., Nakanishi, J., Ijspeert, A.: Learning movement primitives. Springer Tracts in Advanced Robotics **15**, 561–572 (2005). DOI 10.1007/11008941{_}60
46. Shokoohi-Yekta, M., Hu, B., Jin, H., Wang, J., Keogh, E.: Generalizing DTW to the multi-dimensional case requires an adaptive approach. Data Mining and Knowledge Discovery **31**(1), 1–31 (2017). DOI 10.1007/s10618-016-0455-0
47. Sidiropoulos, A., Karayiannidis, Y., Doulgeri, Z.: Human-robot collaborative object transfer using human motion prediction based on dynamic movement primitives. In: 2019 18th European Control Conference, ECC 2019, pp. 2583–2588. Institute of Electrical and Electronics Engineers Inc. (2019). DOI 10.23919/ECC.2019.8796249
48. Sternad, D.: It's not (only) the mean that matters: variability, noise and exploration in skill learning. Current Opinion in Behavioral Sciences **20**, 183–195 (2018). DOI 10.1016/J.COBEHA.2018.01.004
49. Ugur, E., Girgin, H.: Compliant parametric dynamic movement primitives. Robotica **38**(3), 457–474 (2020). DOI 10.1017/S026357471900078X
50. Yang, C., Zeng, C., Fang, C., He, W., Li, Z.: A DMPs-Based Framework for Robot Learning and Generalization of Humanlike Variable Impedance Skills. IEEE/ASME Transactions on Mechatronics **23**(3), 1193–1203 (2018). DOI 10.1109/TMECH.2018.2817589
51. Zhou, Y., Gao, J., Asfour, T.: Movement primitive learning and generalization: Using mixture density networks. IEEE Robotics and Automation Magazine **27**(2), 22–32 (2020). DOI 10.1109/MRA.2020.2980591

View publication stats